MOLECULAR AND CELLULAR BIOLOGY, Nov. 1986, p. 3999–4007
0270-7306/86/113999-09$02.00/0

Vol. 6, No. 11

Varied Interactions between Proviruses and Adjacent Host Chromatin

KATHLEEN F. CONKLIN[1]* AND MARK GROUDINE[1,2]

Division of Basic Sciences, Fred Hutchinson Cancer Research Center, Seattle, Washington 98104,[1] and Department of Radiation Oncology, University of Washington School of Medicine, Seattle, Washington 98195[2]

Received 24 March 1986/Accepted 28 July 1986

Retroviruses integrated at unique locations in the host genome can be expressed at different levels. We have analyzed the preintegration sites of three transcriptionally competent avian endogenous proviruses (*evs*) to determine whether the various levels of provirus expression correlate with their location in active or inactive regions of chromatin. Our results show that in three of four cell types, the chromatin conformation (as defined by relative nuclease sensitivity) of virus preintegration sites correlates with the level of expression of the resident provirus in *ev*$^+$ cells: two inactive proviruses (*ev*-1 and *ev*-2) reside in nuclease-resistant chromatin domains and one active provirus (*ev*-3) resides in a nuclease-sensitive domain. Nuclear runoff transcription assays reveal that the preintegration sites of the active and inactive viruses are not transcribed. However, in erythrocytes of 15-day-old chicken embryos (15d RBCs), the structure and activity of the *ev*-3 provirus is independent of the conformation of its preintegration site. In this cell type, the *ev*-3 preintegration site is organized in a nuclease-resistant conformation, while the *ev*-3 provirus is in a nuclease-sensitive conformation and is transcribed. In addition, the nuclease sensitivity of host sequences adjacent to *ev*-3 is altered in *ev*-3$^+$ 15d RBCs relative to that found in 15d RBCs that lack *ev*-3. These data suggest that the relationship between preintegration site structure and retrovirus expression is more complex than previously described.

Avian and murine retroviruses can be expressed at different levels after integration into the host cell genome (2, 14, 21, 26, 29). In some cases, this variation is not due to genetic differences between the proviruses but instead is dependent on their site of integration (26, 29). Analyses of two mouse mammary tumor virus proviruses acquired by exogenous infection in cultured cells indicated that the differential activity of these proviruses is dependent on their location in nuclease-sensitive or nuclease-resistant regions of the host cell genome (14). An analogous relationship is not evident, however, for murine viruses introduced into the mouse germ line (Mov proviruses; 27, 28). In the latter case, inherited proviruses are inactive, even when located in transcriptionally active regions of chromatin (4, 20). In contrast to Mov proviruses, some of the naturally occurring avian endogenous viruses (*evs*) are active in their inherited chromosomal location (2, 21). We were therefore interested in the relationship between provirus expression and the structure and activity of virus preintegration sites in this system.

The avian endogenous viruses are highly related and stable genetic elements that were introduced into the germ line of chickens during evolution (1, 7, 24, 25, 33). Of the three viruses analyzed in this report, *ev*-1 and *ev*-2 are normally inactive in their inherited locations (producing less than 1 copy of stable RNA per cell; 2, 21), while *ev*-3 is active (producing 50 to 100 copies of stable mRNAs per cell; 2, 21). Previous studies have shown that, while *ev*-3 is hypomethylated and contains the five hypersensitive sites normally found in active proviruses, *ev*-1 and *ev*-2 do not contain either of these features typically associated with active genes (18, 19; unpublished data). These data suggest that the low level of virus-related RNAs detected in *ev*-1- and *ev*-2-containing cells may be due to rare cells in the population that express relatively high levels of RNA rather than to a low-level expression of these proviruses in all cells. For several reasons, the avian *evs* provide a useful system for investigation of the *cis*-interactions between proviral and host DNA that may be involved in determination of gene activity. First, the level of expression of individual proviruses is consistent among different animals and is unaffected by the presence of other endogenous or exogenous viruses in the same cell (21). Second, cloned copies of *ev*-1 and *ev*-2 are transcriptionally active after transfection into chicken embryo fibroblasts (CEFs), even in conjunction with flanking host sequences (10). In addition, *ev*-1 and *ev*-2 are inducible with the methylation inhibitor 5-azacytidine under conditions that are incompatible with mutation (19); under these conditions, *ev*-1 and *ev*-2 are transcribed at approximately the same level as *ev*-3 in untreated cells. These data indicate that *cis*- but not *trans*-acting factors are involved in repression of avian provirus expression, that inactive proviruses are not associated with *cis* inhibitory cellular sequences, that their sites of integration do not preclude transcription under all conditions, and that once activated, all three elements can support transcription at approximately equivalent rates.

Our results show that in three of the four cell types analyzed (MSB-1 cells [a chicken T-cell line transformed by Marek's virus], CEFs, and thymus cells), the transcriptional activity of all three proviruses correlates with the conformation of their preintegration sites. These data indicate that *ev*-1 and *ev*-2 are unable to initiate events required to permit transcription from their inherited chromosomal locations which are in nuclease-resistant inactive regions of chromatin. We also find that in erythrocytes isolated from 15-day-old chicken embryos (15d RBCs), the structure and activity of the *ev*-3 provirus is independent of the conformation of its preintegration site. In addition, the presence of *ev*-3 is

* Corresponding author.

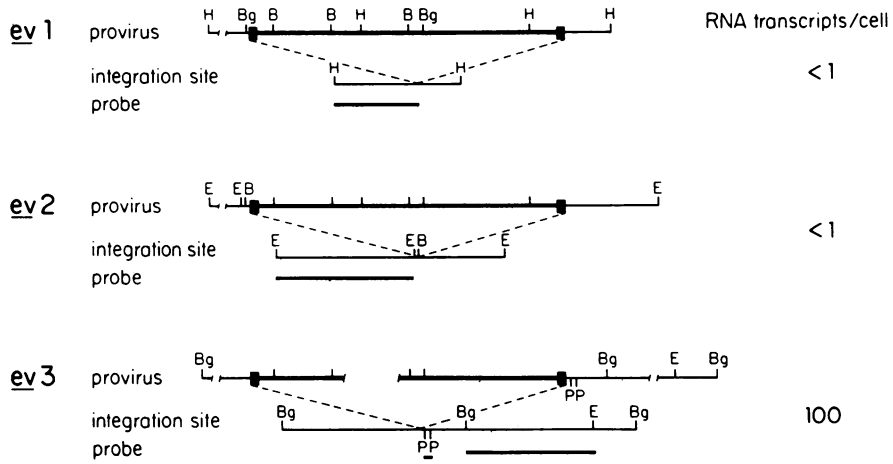

FIG. 1. Partial restriction enzyme maps of *ev*-1, *ev*-2, and *ev*-3 and their integration site regions. Bold lines, proviral DNA; solid boxes, proviral long terminal repeats; and faint lines, cellular DNA. The vertical lines in *ev*-2 and *ev*-3 indicate identical cleavage sites for *Bam*HI (B), *Bgl*II (Bg), and *Hin*dIII (H) marked in *ev*-1. Cleavage sites in host DNAs (E, *Eco*RI; Bg, *Bgl*II) demonstrate the different composition of cellular DNA at each integration site. Dotted lines place the site of provirus insertion in host DNA. Slashed bars in *ev*-3 mark the appropriate location of a deletion in this provirus. RNA transcripts per cell data are from Hayward et al. (21). The host-specific probes used for chromatin analysis and for detection of runoff transcription products are also shown: *ev*-1, a 2.0-kbp *Hin*dIII-*Bgl*II fragment isolated from the cloned 3.3-kbp *Hin*dIII *ev*-1 preintegration site fragment in pGd111 (cloned DNA was a gift of A. Skalka); *ev*-2, a 3.5-kbp *Eco*RI fragment isolated from a cloned copy of *ev*-2 (λ100; a gift of A. Skalka); *ev*-3, 0.3-kbp *Pst*I fragment adjacent to the *ev*-3 integration site and a 3.0-kbp *Bgl*II-*Eco*RI fragment positioned 1 to 5 kbp downstream of the *ev*-3 integration site.

associated with an altered conformation of adjacent host sequences relative to that found in *ev*-3$^-$15d RBC chromatin. Nuclear runoff transcription assays showed that none of the three preintegration site regions were transcribed in any cell type analyzed. These findings indicate that, while chromatin-based regulation may be involved in determining provirus expression in some cases, under certain conditions proviruses can act independently of their integration sites and can be associated with structural alterations in host chromatin as well.

MATERIALS AND METHODS

Cloning the *ev*-3–host junction fragment. Genomic DNA from adult RBC of an *ev*-3$^+$ chicken was digested with *Eco*RI and subjected to electrophoresis in a 1% agarose gel, and DNA between 4 and 6 kilobase pairs (kbp) was excised. This fraction contained an *ev*-3-specific fragment of 5.0 kbp which includes approximately 1.4 kbp of proviral DNA and 3.6 kbp of host DNA downstream of *ev*-3 (24). DNA was purified from the gel slice and subsequently ligated with *Eco*RI-cleaved λgt10. Positive plaques obtained from in vitro-packaged ligation products were detected with virus-specific probes. A partial map of the *ev*-3–host junction fragment is shown in Fig. 1.

Cells and nucleus isolation. The 15d RBCs were obtained by vein puncture, and nuclei were isolated as previously described (38). MSB-1 cells were a gift of M. Linial and C. Thompson. CEF from virus-free C/O embryos were a gift of M. Linial and B. Biegalke. Ficoll-Hypaque-purified thymus cells were prepared as previously described (40). Nucleus isolation from RBCs, CEFs, and MSB-1 and thymus cells was conducted as previously described (38, 40), except that for CEFs, lysis was accomplished in reticulocyte standard buffer–0.5% Nonidet P-40 by disruption in a Dounce homogenizer.

Nuclease digestion. Nuclease digestion series were generated from 15d RBCs, MSB-1 cells, and CEFs by incubating aliquots of nuclei with increasing concentrations of DNase I as previously described (38). Nuclease digestion of thymus nuclei, which have a high concentration of endogenous nuclease, was accomplished by incubating aliquots of nuclei for increasing periods at 37°C.

Restriction endonuclease digestion, gel electrophoresis, transfer to nitrocellulose, and filter hybridizations were conducted as previously described (38).

To establish the relative nuclease sensitivity of cellular genes, care was taken to avoid fragments that contained major internal nuclease-hypersensitive sites. Listed below are the restriction enzymes used to digest nuclease-treated genomic DNA, fragments from cloned DNAs used for probes, and references that include restriction enzyme or nuclease-hypersensitive maps or both; histone H2b, *Sac*I plus *Xho*I, 450-base-pair (bp) *Dra*I-*Sac*II fragment (cloned DNA was a gift of P. Krieg) (11); thymidine kinase, *Hin*dIII plus *Kpn*I, 2.9-kbp *Hin*dII-*Hin*dIII fragment (cloned DNA was a gift of M. Wigler) (17); *myc*, *Sac*I, 3.2-kbp *Sac*I-*Sac*I fragment (32, 35); actin, *Bam*HI plus *Hin*dIII, 590-bp *Pst*I fragment (plasmid pA2) (6); α-globin, *Bam*HI plus *Hin*dIII, three *Bam*HI fragments of 1.5, 1.9, and 3.0 kbp which include coding regions for α^D and α^A and a noncoding region downstream of the coding regions, respectively (12, 42); and vitellogenin II (VTGII), *Bam*HI, 3.7-kbp *Bam*HI-*Bam*HI fragment (plasmid VTG412; cloned DNA was a gift of J. Burch) (5). There are several copies of the H2b gene in the chicken genome. Coding portions of the actin gene also hybridize to several distinct regions. To ensure that we were analyzing one discrete fragment in each case, probes utilized contained sequences located either immediately downstream of coding sequences (H2b) or in a transcribed but nontranslated portion of the coding region (actin), each of which is unique to one locus. Cell-specific probes used to detect individual preintegration site regions are depicted in each figure.

Nuclear Runoff transcription, RNA isolation, and analysis. Transcription reactions, DNA slot blots, and hybridization

reactions were performed as described previously (31). The plasmids used contained the following inserts: Myc, a 2.4-kbp *Sac*I-*Eco*RI fragment that includes the second and third *myc* exons (32); GAPDH, a 1.2-kbp fragment from a partial cDNA clone (13); H2b, a 650-bp *Hin*dIII-*Dra*I fragment that includes the entire coding region of H2b (11; P. Challoner, personal communication); α^D, a 1.1-kbp *Bam*HI fragment that includes 0;7 kbp of α^D coding region and 0.4 kbp of DNA upstream of α^D (12); and VTGII a 3.7-kbp *Bam*HI fragment from within the chicken vitellogenin II gene (5). Viral sequences were detected with plasmids that contained the following: *gag*, a 1.8-kbp *Bam*HI fragment specific for the viral *gag* structural gene; *env*, a 2.1-kbp *Bam*HI-*Xba*I fragment from within the viral *env* gene (obtained from E. Hunter); 5′ virus, containing a 3.0-kbp *Eco*RI fragment that includes approximately 2.7 kbp of viral DNA and 300 bp of host DNA (this fragment is a portion of the integrated *ev*-2 provirus) (34); 3′ virus, derived from the 5.0-kbp *Eco*RI *ev*-3–host junction fragment (Fig. 1) and containing a 2-kbp insert, one end of which is defined by the *Eco*RI site in proviral DNA and the other end of which is defined by a *Bgl*II site in adjacent host cellular DNA. We used between 2 and 7 μg of plasmid DNA per slot and obtained identical results in repeat experiments, indicating that these amounts represent DNA excess for all genes examined.

RESULTS

Transcriptional activity of *ev*-1 and *ev*-3 in thymus cells. Figure 2 shows the difference in transcriptional activity of *ev*-1 and *ev*-3 as determined by nuclear runoff transcription assays with thymus-derived nuclei. As shown, runoff transcripts from the single-copy *myc* gene were present in both the *ev*-1 and *ev*-1+3 samples. However, while both *gag*- and *env*-related products were detectable in *ev*-3-containing cells, we were unable to detect any transcription of these regions in cells containing only *ev*-1, even after long overexposures. Additional experiments showed that *ev*-1 is also inactive, as determined by nuclear runoff assays with MSB-1 cells (see also reference 20), and that both *ev*-1 and *ev*-2 are inactive in CEFs (data not shown). Previous mixing experiments have shown that a transcription signal from *ev*-3 is readily detectable when only 10% of the nuclei in the assay contain this provirus (unpublished). In addition, other transcriptionally active cellular genes (e.g., c-*myb*) give hybridization signals approximately 10-fold lower than that observed with *ev*-3 (41), indicating that the activity of *ev*-3 does not represent a lower limit of detection in this assay. Our failure to detect transcripts from *ev*-1 and *ev*-2 therefore most probably represents the absence of elongating polymerases along these proviruses. Thus, these data demonstrate that in each cell type analyzed, *ev*-1, *ev*-2, and *ev*-3 are expressed at a characteristic level which corresponds to the steady-state levels of virus-related RNA in CEFs that contain these proviruses (2, 21).

Relative nuclease sensitivity of cellular chromatin associated with *ev*-1, *ev*-2, and *ev*-3. Figure 1 includes partial restriction enzyme maps of the three proviruses and proviral integration sites analyzed together with the host-specific DNA fragments used to detect each locus. To determine the relative level of nuclease sensitivity of provirus preintegration sites, Southern blots were generated from restriction enzyme-digested DNAs that had been purified from nuclease-digested thymus nuclei; identical experiments were also performed with other cell types including MSB-1 cells, CEFs, and, for *ev*-1, liver cells. Individual filters were hybridized with probes specific for the integration site regions of *ev*-1, *ev*-2, and *ev*-3, as well as with probes which detect one of several active cellular genes or the liver-specific VTGII gene (which is inactive in thymus cells; see below). To monitor the general sensitivity of each region, we chose restriction enzyme-probe combinations that generated fragments devoid of major internal nuclease-hypersensitive sites (see Materials and Methods for details). This is an important consideration, since cleavage at hypersensitive sites leads to the rapid disappearance of a full-length restriction fragment and therefore obscures differences in overall sensitivity.

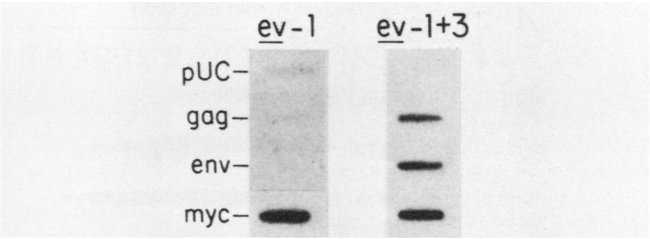

FIG. 2. Transcriptional activity of *ev*-1 and *ev*-3 in thymic nuclei. Radiolabeled runoff transcription products obtained from thymus nuclei were hybridized to plasmid DNAs immobilized on nitrocellulose filters that contained inserts of the viral *gag* and *env* genes and the cellular *myc* gene as described in Materials and Methods.

The 3.7-kbp fragment that includes a portion of the inactive VTGII gene was highly resistant to nuclease digestion relative to fragments generated from the active H2b, *myc*, actin, and *tk* genes (Fig. 3). Several chicken globin genes were also nuclease resistant in this cell type (data not shown). Since larger DNA fragments, owing to their greater target size for nuclease cleavage, are digested faster than small fragments and since the VTGII fragment (3.7 kbp) is larger than those analyzed from H2b (1.1 kbp), *myc* (3.2 kbp), and *tk* (2.1 kbp), the insensitivity of the VTGII gene-derived fragment demonstrated that this nuclease digestion series allowed a clear distinction between nuclease-sensitive and nuclease-resistant regions of chromatin.

The lower portion of Fig. 3A shows the rate of digestion of host regions associated with *ev*-1, *ev*-2, and *ev*-3 in thymic cells; Fig. 3B includes partial maps of each region together with probes used for this analysis. These thymus cells were derived from animals that were homozygous for *ev*-1; the 4.5-kbp *Hin*dIII fragment therefore includes 2-kbp of host DNA upstream of *ev*-1 and 2.5 kbp of proviral DNA (36). As previously described (20), *ev*-1 lacks all nuclease-hypersensitive sites found in active proviruses. Comparison of the rate of digestion of this fragment with that of the active and inactive genes shown above demonstrates that the *ev*-1–host fragment is as resistant to nuclease digestion as is the VTGII gene-derived fragment. Additional experiments revealed that this conformation extends at least 10 kbp on either side of the *ev*-1 integration site in all cell types tested (data not shown). In addition, the *ev*-1 preintegration site is organized in a highly resistant conformation. This is depicted in Fig. 3C, which shows that in CEFs obtained from an animal that was heterozygous for *ev*-1, *Hin*dIII fragments that represent the *ev*-1$^+$ (4.5 kbp) and the *ev*-1$^-$ (3.3 kbp) alleles (Fig. 3D) are equally resistant to nuclease digestion. Additional analyses of regions that contained active and inactive control genes in these CEF-derived nuclei showed characteristic differences in sensitivity (data not shown).

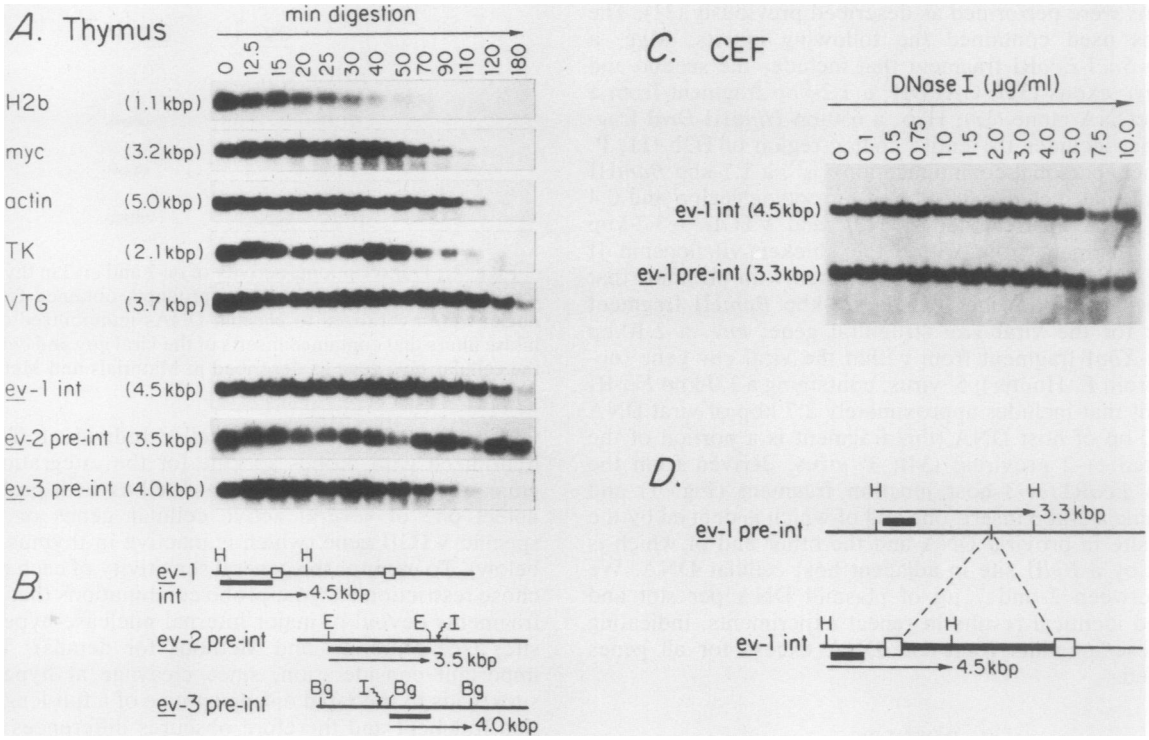

FIG. 3. Relative levels of nuclease sensitivity of host regions associated with *ev*-1, *ev*-2, and *ev*-3 as analyzed in thymus- and CEF-derived chromatin. A nuclease digestion series was generated with nuclei isolated from thymus cells as described in Materials and Methods. (A) Each band represents a portion of individual autoradiographs obtained with probes specific for histone H2b (H2b), the cellular *myc* gene (myc), cytoplasmic actin gene (actin), the chicken *tk* gene (TK), and the chicken vitellogenin II gene (VTG). Restriction enzymes and probes used for cellular genes are listed in Materials and Methods; those used for provirus integration sites are shown in panel B. The thymus cells used in this example were isolated from animals that contained *ev*-1. Therefore, the 4.5-kbp *Hin*dIII fragment detected by the 2.0-kbp *Hin*dIII-*Bgl*II probe includes approximately 2.0 kbp of host DNA flanking *ev*-1 plus approximately 2.5 kbp of *ev*-1 proviral DNA (Fig. 1 and line drawing in panel B). The *ev*-2 preintegration site-specific fragment was generated by *Eco*RI digestion of cellular DNA and was detected by hybridization with the 3.5-kbp *Eco*RI fragment. For the *ev*-3 preintegration site, digestion was with *Bgl*II. The fragment shown in panel A is the 4.0-kbp *Bgl*II product downstream of the *ev*-3 integration site; identical results were obtained with the 0.3-kbp *Pst*I probe specific for a 4.0-kbp *Bgl*II fragment that spans the *ev*-3 integration site. (C) A nuclease digestion series was generated with CEFs derived from an animal that was heterozygous for *ev*-1. Purified DNA was digested with *Hin*dIII and Southern blots were probed with the same *ev*-1-specific *Hin*dIII-*Bgl*II probe used in panel A. The 4.5-kbp band is the provirus-host junction fragment, while the 3.3-kbp band is the *ev*-1 preintegration site (see line drawing in panel D). Additional control experiments (data not shown) demonstrated that active and inactive regions showed characteristic differences in nuclease sensitivity. None of the fragments included in this analysis contained major hypersensitive sites. H, *Hin*dIII; E, *Eco*RI; Bg, *Bgl*II. I denotes the location of provirus integration in host DNA.

This demonstrates that insertion of proviral DNA neither induces this resistant conformation nor leads to any detectable changes in the organization of adjacent host chromatin.

Analyses of *Eco*RI-digested DNAs purified from nuclease-digested thymus nuclei (Fig. 3A), MSB-1 cells, or CEFs (data not shown) showed that host chromatin from 3.1 to 0.3 kbp upstream of the integration site of the inactive *ev*-2 provirus was also organized in a highly nuclease-resistant conformation in *ev*-2$^-$ cells.

To determine the rate of digestion of fragments which either span the *ev*-3 integration site or are located 1 to 5 kbp downstream of *ev*-3, DNA obtained from nuclease-digested nuclei was restricted with *Bgl*II and probed with either the 0.3-kbp *Pst*I fragment or the 3.0-kbp *Bgl*II-*Eco*RI fragment shown in Fig. 1. Results obtained with each fragment were identical; those obtained with thymus samples and the 3.0-kbp probe are shown in Fig. 3A. A comparison of the rate of digestion of the *ev*-3 preintegration site fragment with those derived from active and inactive genes showed that it was significantly more sensitive to digestion than were resistant regions and that the rate of digestion more closely paralleled the rate for regions containing the transcriptionally active *myc*, actin, and *tk* genes.

These results demonstrate that in chromatin of thymus cells, CEFs, and MSB-1 cells, the preintegration sites of inactive and active endogenous proviruses are conformationally distinct and that these differences are consistent with the activity of the integrated proviruses.

Transcriptional activity of host DNA associated with *ev*-1 and *ev*-3. A nuclease-sensitive conformation is not limited to regions of chromatin that are actively transcribed; regions of chromatin adjacent to transcribed sequences are also more sensitive to nuclease digestion than bulk (i.e., inactive) chromatin (42). Therefore, to determine whether the conformation of the *ev*-3 preintegration site was indicative of transcription, we performed nuclear runoff assays with nuclei isolated from thymus cells, MSB-1 cells, and CEFs. Radiolabeled RNAs were purified and used to probe filters that contained plasmid DNAs with inserts from several control genes and from host DNA associated with *ev*-1 and

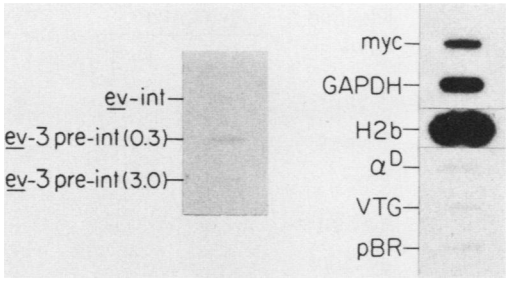

FIG. 4. Runoff transcription products from thymus nuclei. Radiolabeled runoff transcription products obtained from the thymus nuclei used in Fig. 2 were hybridized with plasmid DNAs immobilized on nitrocellulose filters as described in Materials and Methods.

ev-3. Results obtained with the thymus-derived nuclei are shown in Fig. 4; identical results were obtained with CEFs and MSB-1 cells (data not shown). As shown, RNAs homologous to the single-copy *myc* and GAPDH genes were easily detectable by this technique, as were transcripts of the multicopy histone H2b gene. We detected no signal above that obtained with pBR322 to plasmids containing either the liver-specific VTGII gene or the RBC-specific α^D globin gene. Plasmids that contained the 3.0- and 0.3-kbp host fragments downstream of *ev*-3 were each used to monitor the transcriptional activity of the *ev*-3 preintegration site. No signal above the pBR322 control was detectable with either plasmid (Fig. 4). Owing to the relative nuclease sensitivity of this region (Fig. 3A; data not shown), this result indicates that the *ev*-3 preintegration site is organized in a conformation compatible with transcription but that it does not include transcribed sequences.

Chromatin conformation of *ev*-3 and its preintegration site in 15d RBCs. In the course of these analyses, we identified one cell type, 15d RBCs, in which the *ev*-3 preintegration site was organized in a nuclease-resistant conformation relative to control genes. The fragments analyzed in this series were the same as those described in Fig. 3A, with two exceptions (Fig. 5A). First, this embryo lacked all *ev*-related sequences (*ev*-0 bird). Therefore, the *ev*-1-associated region is represented by a 3.3-kb *Hin*dIII fragment that spans the virus integration site (Fig. 1). Second, in place of using H2b, we analyzed the relative sensitivity of several regions of the RBC-specific α-globin locus.

As shown in the top three panels, the globin gene probe detected three fragments: the 1.9- and 1.5-kbp bands include

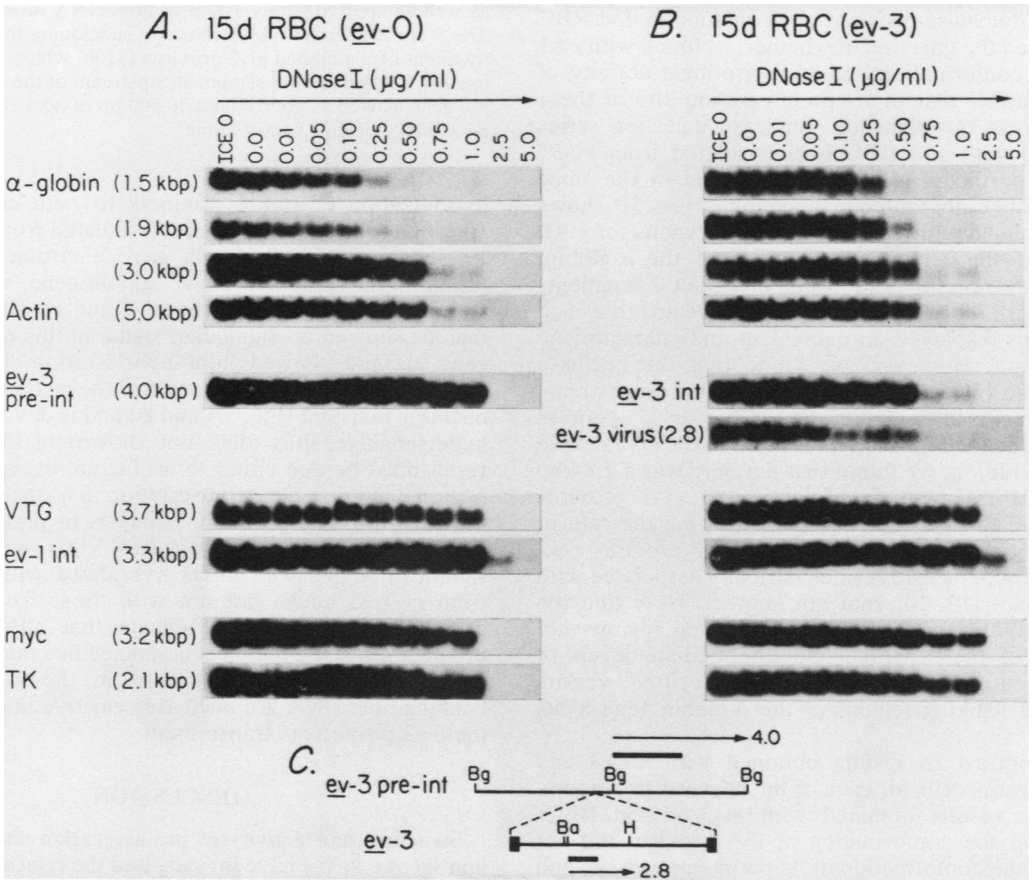

FIG. 5. Relative levels of nuclease sensitivity in 15d embryonic RBC chromatin of several cellular genes, of the *ev*-1 and *ev*-3 integration site regions, and of the *ev*-3 provirus. DNase I digestion series were generated with nuclei obtained from 15d RBCs that either lacked all *ev*-related sequences (A; *ev*-0) or were homozygous for *ev*-3 (B; *ev*-3), as described in Materials and Methods. Restriction enzyme digestion and probing strategies for actin, *ev*-3 pre-int, VTGII, *ev*-1 pre-int, *myc*, and *tk* were the same as for Fig. 3; details for these genes and the α-globin regions are described in Materials and Methods. Note that in each of these samples, which do not contain *ev*-1, the *ev*-1-specific fragment is the 3.3-kbp *Hin*dIII fragment that spans the *ev*-1 integration site (Fig. 1). The line drawing in panel C depicts both the 2.8-kbp *ev*-3 virus fragment which was generated by *Bam*HI plus *Hin*dIII digestion of genomic DNA and the 4-kbp *Bgl*II fragment downstream of *ev*-3.

the coding regions of the α^A and α^D genes, respectively, and the 3.0-kbp fragment is a nontranscribed region approximately 2 kbp downstream of the α-globin coding region (11, 42). Comparison of the rates of digestion of the α-globin and VTGII fragments in 15d RBCs showed a clear distinction between the DNase I-resistant, inactive VTGII gene, the DNase I-sensitive, transcriptionally active α-globin genes, and the intermediate-sensitive, nontranscribed segment adjacent to the α-globin gene cluster. In agreement with results obtained for non-RBC chromatin (Fig. 3C, data not shown), the *ev*-1 preintegration site region was as resistant to nuclease digestion as was the inactive VTGII gene, while the actin gene was considerably more sensitive to nuclease digestion than these inactive regions. We also analyzed 15d RBCs from *ev*-1-containing animals and found that the provirus is as resistant to nuclease digestion as are both the VTG gene and the *ev*-1 preintegration site region (data not shown). However, in contrast to results described above, the rate of digestion of the *ev*-3 preintegration site region, as well as fragments including the *myc* and *tk* genes, closely paralleled that of the inactive VTGII gene. Additional analyses (data not shown) revealed that the characteristic c-*myc* hypersensitive sites present in all other cell types (including chromatin from 9d embryonic RBCs) as well as myc related transcripts (see below) were absent in 15d embryonic RBCs.

The finding that the *ev*-3 preintegration site region is organized in a nuclease-resistant conformation in 15d RBC chromatin raised the question of whether, as found with *ev*-1 and *ev*-2, the conformation and transcriptional activity of *ev*-3 would parallel that of its preintegration site in these cells. To address this question, nuclease digestion series were prepared with 15d RBC nuclei isolated from *ev*-3^+ embryos and purified DNAs were subjected to the same analyses described above for *ev*-0 samples; Fig. 5B shows the results obtained with one embryo homozygous for *ev*-3. Comparison of the relative sensitivities of the α-globin, actin, VTGII, *ev*-1 preintegration site, *myc*, and *tk* fragments in this series with those shown in Fig. 5A revealed that each of these regions displayed an equivalent and characteristic rate of digestion. However, we found that the nuclease sensitivity of the 4.0-kbp *Bgl*II fragment located downstream of *ev*-3 was increased significantly in the *ev*-3^+ samples relative to that defined for the same region in the *ev*-0 sample (Fig. 5A). In addition, we found that not only was a 2.8-kbp *Bam*HI-*Hin*dIII fragment from within the *ev*-3 provirus highly sensitive to digestion, closely following the rate of α-globin coding sequences, but also the *ev*-3 provirus contained the five hypersensitive sites normally associated with active proviruses (19, 20; data not shown). Note that the relative sensitivities of proviral and flanking regions are characteristic of the sensitive and intermediate levels of nuclease digestion seen for the transcribed versus nontranscribed flanking regions of the α-globin gene locus (42).

Thus, in contrast to results obtained with CEFs and MSB-1 and thymus cells for each of the provirus preintegration sites, the results obtained with *ev*-3 in 15d RBCs indicate (i) that the conformation of this provirus did not correlate with the conformation of its preintegration site and (ii) that the presence of *ev*-3 was associated with a change in the conformation of flanking cellular chromatin.

Transcriptional activity of *ev*-3 in 15d RBCs. To determine whether the active conformation of *ev*-3 in 15d RBCs was indicative of transcription of the provirus, nuclear runoff transcription assays were conducted with nuclei obtained from *ev*-1 and *ev*-1+3 RBCs. Figure 6 shows the pattern of hybridization of runoff products to both cell- and virus-specific probes. Runoff products isolated from *ev*-1- and *ev*-1+3-containing nuclei each gave a strong signal with a plasmid that contained the α^D globin gene, while the liver-specific VTGII gene and the *ev*-1 and *ev*-3 integration site regions showed no significant signal in this assay. The *myc* gene plasmid showed faint hybridization; in light of our chromatin results, which show that the *myc* gene is relatively nuclease resistant (Fig. 5A and B) and is devoid of nuclease-hypersensitive sites (data not shown) in these cells, this result must be due either to artifactual background hybridization or to *myc* gene transcription in a small percentage of the cells in the population. Analysis of plasmids that contained viral sequences (3′ virus, 5′ virus, and *env*) showed significant signal with filters hybridized with runoff RNAs from *ev*-1+3 nuclei but not with those from *ev*-1 nuclei. Therefore, these results indicate that although the *ev*-3 preintegration site region is organized in a nuclease-resistant conformation in 15d RBC chromatin, the *ev*-3 provirus and flanking host DNA are nuclease sensitive in *ev*-3^+ cells and the *ev*-3 provirus is transcribed.

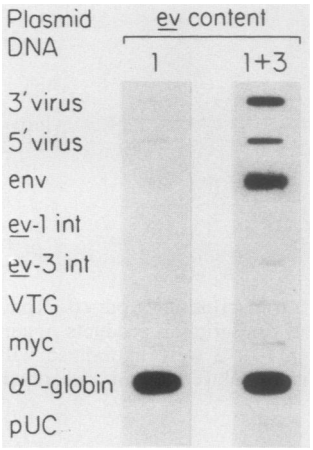

FIG. 6. Analysis of nuclear runoff transcription products from *ev*-1 and *ev*-1+3 15d RBCs. Radiolabeled runoff transcription products obtained from either *ev*-1- or *ev*-1+3-containing 15d RBC nuclei were hybridized to plasmid DNAs immobilized on nitrocellulose filters as described in Materials and Methods. The *ev*-3 int specific plasmid used here contained the 3.0-kbp *Bgl*II-*Eco*RI fragment downstream of *ev*-3 (Fig. 1). The 3′ virus plasmid was generated from the cloned *ev*-3 provirus and includes all *env* and long terminal repeat sequences downstream of the *Eco*RI site in the viral *env* gene as well as approximately 1 kbp of host DNA downstream of *ev*-3. The 5′ virus plasmid was derived by subcloning the 3.5-kbp *Eco*RI fragment of the cloned *ev*-2 provirus (λ100) which includes approximately 2.9 kbp of viral sequences upstream of the *Eco*RI site in the *pol* gene as well as approximately 300 bp of host DNA upstream of *ev*-2. pUC, pUC18 vector alone.

DISCUSSION

Structure and activity of preintegration sites of expressed and silent *ev*s. We have investigated the relationship between the expression of several avian *ev*s and the conformation and activity (as defined by relative nuclease sensitivity and nuclear runoff transcription) of their respective preintegration sites. Our results showed that, as measured by nuclear runoff assays, virus-related transcription products were readily detectable in all *ev*-3^+ cells (including thymus and bursa cells, CEFs, and 15d RBCs). We were unable to detect

provirus-encoded transcripts in identical cell types, in MSB-1 cells that contained only *ev*-1, or in *ev*-2-containing CEFs. These data are consistent with the previously reported levels of steady-state virus-related RNAs in *ev*-1-, *ev*-2-, and *ev*-3-containing CEFs (2, 21).

Our characterization of virus preintegration sites revealed that host regions associated with *ev*-1 and *ev*-3 were transcriptionally inactive as measured by nuclear runoff assays in several cell types; no change in activity of these host regions was detected in cells that contained the proviruses. These data demonstrate that transcription of provirus preintegration sites per se is not related to the subsequent activity of the integrated proviruses. We also found, however, that in three of four cell types analyzed, the level of expression of each *ev* did correlate with the conformation of its preintegration site: two inactive proviruses (*ev*-1 and *ev*-2) were located in nuclease-resistant chromatin domains, while the preintegration site of the active *ev*-3 provirus was nuclease sensitive. In the fourth cell type, 15d RBCs, this correlation was not evident. In these cells, *ev*-3 was transcriptionally active and was organized in a nuclease-sensitive conformation, while its preintegration site was highly resistant to nuclease digestion. In addition, host DNA adjacent to *ev*-3 was significantly more sensitive to digestion that was this same region in *ev*-3$^-$ 15d RBCs. Our results with *ev*-1 and *ev*-2 and with *ev*-3 in non-RBC chromatin support a role for chromatin-based regulation of provirus expression, which has been proposed previously to account for the differential expression of two mouse mammary tumor virus proviruses in cultured cells (14). This type of regulation also has been well documented in the differential expression of genes associated with DNA rearrangements, including those that involve either inactive copies of the X chromosome or centromeric and perhaps telomeric regions of the *Drosophila* genome (reviewed in references 3, 9, 15, and 37; see also references 22 and 30). In these cases, genes that are expressed in their normal locations can be transcriptionally inactivated and can adopt the inactive conformation of the region into which they are placed. This model is inadequate, however, to explain our observation that in 15d RBCs, *ev*-3 can act independently and can overcome host factors which operate on its preintegration site in these cells.

Possible mechanisms for these interactions. There are several possible explanations for these results. The first is that the apparent dominance of *ev*-3 over host factors in 15d RBCs reflects genetic differences between *ev*-3 and *ev*-1 and *ev*-2. We have sequenced a portion of the *ev*-3 long terminal repeat required for transcription (the U3 region) and found a 3-bp difference from the published sequence of *ev*-1 (23); one of these changes is also found for *ev*-2 (34). While these are minor differences, it is possible that they account for the activity of *ev*-3 in 15d RBCs. We are currently investigating the potential functional significance of these changes in sequence.

Another possibility is that the positive correlations between the conformation of virus preintegration sites and subsequent provirus expression are due to factors other than chromatin structure (such as DNA methylation), which are frequently, but not exclusively, associated with active or inactive regions of chromatin. For example, we previously reported that *ev*-1 is highly methylated, while *ev*-3 is not (8, 18, 19). In addition, both *ev*-1 and *ev*-2 are inducible with the methylation inhibitor 5-azacytidine (19; unpublished data), indicating that methylation plays a role in at least maintaining provirus repression. Preliminary analyses have shown that the pre- (and post-) integration sites of *ev*-1 are highly methylated, while the *ev*-3 preintegration site contains hypomethylated sites in all cell types analyzed (including 15d RBCs). Thus, one formal possibility is that the partially methylated state, rather than the chromatin structure per se of the *ev*-3 preintegration site, is the important factor in permitting expression of *ev*-3 at this location.

Finally, it is possible that, while exogenously acquired proviruses may be subject to chromatin-based regulation in the originally infected cell type, proviruses inherited through the germ line may show cell type-specific differences in their interactions with flanking host regions. Such differences could depend on the developmentally regulated events that affect either the conformation or activity of proviral or integration site-specific regions. In this regard, we find it interesting that the only cell type identified which contains the *ev*-3 preintegration site in a nuclease-resistant conformation is 15d RBC. The potential significance of this finding is suggested by the fact that RBC chromatin undergoes considerable condensation during maturation of immature erythroblasts to the more mature erythrocytes analyzed in the work described in this report (16). Our analysis of the *myc* gene has shown that its inactivation during erythropoiesis is coincident with this condensation: characteristic hypersensitive sites normally associated with *myc* in the less-mature population of RBCs present at 9 to 10 days of development are no longer detectable in 15d RBCs, which consist predominantly of mature cells with condensed nuclei (16). This condensation is accompanied by transcriptional inactivation of *myc*. These data raise the very likely possibility that the nuclease-resistant conformation of the *ev*-3 preintegration site in 15d RBCs is also a result of this condensation. Since the *ev*-3 preintegration site is not transcribed and does not contain nuclease-hypersensitive sites, it is necessary to separate immature RBCs from the mixed population of cells present in circulating blood to establish the conformation of this region in precursor cells. This will allow us to determine whether the presence (and continued transcription) of *ev*-3 blocks the condensation that normally occurs in its preintegration site or whether integration of *ev*-3 actively induces chromatin changes in cells of the erythroid lineage.

Comparison of avian and murine proviruses inherited through the germ line. Studies similar to those described here have also been conducted with murine leukemia viruses introduced into the mouse germ line (Mov proviruses; 4, 20, 27, 28). A comparison of these two systems indicates that, while certain similarities exist, the expression of avain and murine viruses that are inherited through the germ line is regulated by different mechanisms. This is suggested by several findings. First, all inherited Mov proviruses are reportedly transcriptionally inactive in each cell type analyzed (27). Second, one provirus (Mov 13) is inactive even in cells that normally express its preintegration site (which is within the mouse α1(I)-collagen gene; 4, 20). Third, all Mov proviruses are heavily methylated and can be associated with increased methylation of flanking host DNA (28, 39). Together, these data indicate that Mov proviruses introduced into mouse embryos prior to preimplantation appear to be inactivated early in development and that this repression is not only maintained at later stages but can also spread to include adjacent host DNA. In contrast to these results, both active and inactive avian *evs* have been identified (even in the same cells of a given animal), and the level of methylation of individual proviruses is consistent with their level of expression (18, 19; unpublished data). Thus, these data indicate that, in apparent contrast to mice, chickens do

not have a mechanism to inactivate all *ev*s, or that, if present, this inactivation is not maintained at all locations as it is during mouse development.

ACKNOWLEDGMENTS

We thank Mary Peretz, Angela Hein, and Hal Hendron for expert technical assistance and Helen Devitt for help in preparing the manuscript. We also thank Hal Weintraub, Craig Thompson, Maxine Linial, and other members of the Hutchinson Center for their comments and suggestions during the course of this work. Cloned copies of the provirus-host junction fragments of *ev*-1 and *ev*-2 and of the *ev*-1 preintegration site were kindly provided by A. M. Skalka.

This work was supported by National Science Foundation grant PCM 82-04696 (to M.G.) and a Scholarship (to M.G.) and a Special Fellowship (to K.F.C.) from the Leukemia Society of America.

LITERATURE CITED

1. **Astrin, S. M., H. L. Robinson, L. B. Crittenden, E. G. Buss, J. Wyban, and W. S. Hayward.** 1980. Ten genetic loci in the chicken that contain structural genes for endogenous avian leukosis viruses. Cold Spring Harbor Symp. Quant. Biol. **44**:1105–1109.
2. **Baker, B., H. L. Robinson, H. E. Varmus, and J. M. Bishop.** 1981. Analysis of endogenous avian retrovirus DNA and RNA: viral and cellular determinants of retrovirus gene expression. Virology **114**:8-22.
3. **Baker, W. K.** 1968. Position-effect variegation. Adv. Genet. **14**:113–169.
4. **Briendl, M., K. Harbers, and R. Jaenisch.** 1984. Retrovirus-induced lethal mutation in collagen I gene of mice is associated with an altered chromatin structure. Cell **38**:9–16.
5. **Burch, J. B. E., and H. Weintraub.** 1983. Temporal order of chromatin structural changes associated with activation of the major chicken vitellogenin gene. Cell **33**:65–76.
6. **Cleveland, D. W., M. A. Lopata, R. J. MacDonald, N. J. Cowan, W. J. Rutter, and M. W. Kirschner.** 1980. Number and evolutionary conservation of α- and β-tubulin and cytoplasmic β- and γ-actin genes using specific cloned cDNA probes. Cell **20**:95–105.
7. **Coffin, J. M., P. N. Tsichlis, K. F. Conklin, A. M. Senior, and H. L. Robinson.** 1983. Genomes of endogenous and exogenous avian retroviruses. Virology **15**:51–72.
8. **Conklin, K. F., J. M. Coffin, H. L. Robinson, M. Groudine, and R. Eisenman.** 1982. Role of methylation in the induced and spontaneous expression of the avian endogenous virus *ev*-1: DNA structure and gene products. Mol. Cell. Biol. **2**:638–652.
9. **Conklin, K. F., and M. Groudine.** 1984. Chromatin structure and gene expression, p. 293–351. *In* A. Razin, H. Cedar, and A. D. Riggs (ed.), DNA methylation. Springer-Verlag, New York.
10. **Cullen, B. R., K. Raymond, and G. Ju.** 1985. Transcriptional activity of avian retroviral long terminal repeats directly correlates with enhancer activity. J. Virol. **53**:515–521.
11. **D'Andrea, R. J., L. S. Coles, C. Lesnikowski, L. Tabe, and J. R. E. Wells.** 1985. Chromosomal organization of chicken histone genes: preferred associations and inverted duplications. Mol. Cell. Biol. **5**:3108–3115.
12. **Dodgson, J., and J. D. Engel.** 1980. Analysis of the closely linked adult chicken α-globin genes in recombinant DNAs. Proc. Natl. Acad. Sci. USA **77**:2596–2599.
13. **Dugaiczyk, A., J. A. Haron, E. M. Stone, O. E. Dennison, K. N. Rothblum, and R. J. Schwartz.** 1983. Cloning and sequencing of a deoxyribonucleic acid copy of glyceraldehyde-3-phosphate dehydrogenase messenger ribonucleic acid isolated from chicken muscle. Biochemistry **22**:1605–1613.
14. **Feinstein, S. C., S. R. Ross, and K. R. Yamamoto.** 1982. Chromosomal position effects determine transcriptional potential of integrated mammary tumor virus DNA. J. Mol. Biol. **156**:549–565.
15. **Gartler, S. M., and A. D. Riggs.** 1983. Mammalian X-chromosome inactivation. Annu. Rev. Genet. **17**:155–190.
16. **Gasaryan, K. G.** 1982. Genome activity and gene expression in avian erythroid cells. Int. Rev. Cytol. **74**:95–126.
17. **Groudine, M., and C. Casmir.** 1984. Post-transcriptional regulation of the chicken thymidine kinase gene. Nucleic Acids Res. **12**:1427–1445.
18. **Groudine, M., and K. F. Conklin.** 1985. Chromatin structure and de novo methylation of spern DNA: implications for activation of the paternal genome. Science **228**:1061–1068.
19. **Groudine, M., R. Eisenman, and H. Weintraub.** 1981. Chromatin structure of endogenous retroviral genomes and activation by an inhibitor of DNA methylation. Nature (London) **292**:311–317.
20. **Harbers, K., M. Kuehn, H. Delius, and R. Jaenisch.** 1984. Insertion of retrovirus into the first intron on α1(I) collagen gene leads to embryonic lethal mutation in mice. Proc. Natl. Acad. Sci. USA **81**:1504–1508.
21. **Hayward, W. S., S. B. Braverman, and S. M. Astrin.** 1980. Transcriptional products and DNA structure of endogenous avian proviruses. Cold Spring Harbor Symp. Quant. Biol. **44**:1111–1121.
22. **Hazelrigg, T., R. Levis, and G. M. Rubin.** 1984. Transformation of *white* locus DNA in *Drosophila*: dosage compensation, *zeste* ineraction, position effects. Cell **36**:460–481.
23. **Hishinuma, F., P. J. DeBona, S. Astrin, and A. M. Shalka.** 1981. Nucleotide sequence of the acceptor site and termini of integrated avian endogenous provirus *ev*-1: integration creates a 6 bp repeat of host DNA. Cell **23**:155–164.
24. **Hughes, S. H., K. Taysoshima, J. M. Bishop, and H. E. Varmus.** 1981. Organization of the endogenous proviruses of chickens: implications for origin and expression. Virology **108**:189–207.
25. **Hughes, S. H., P. K. Vogt, J. M. Bishop, and H. E. Varmus.** 1981. Endogenous proviruses of random-bred chickens and ring-necked pheasants: analysis with reaction endonucleases. Virology **108**:222–229.
26. **Humphries, E. H., R. Allen, and C. Glover.** 1981. Clonal analysis of the integration and expression of endogenous avian retrovirus DNA acquired by exogenous viral infection. J. Virol. **39**:584–596.
27. **Jaenisch, R., D. Jahner, P. Nobis, I. Simon, J. Lohler, K. Harbers and D. Grotkopp.** 1981. Chromosomal position and activation of retrovirus genomes inserted into the germ line of mice. Cell **24**:519–529.
28. **Jahner, D., and R. Jaenisch.** 1985. Retrovirus-induced de novo methylation of flanking host sequences correlates with gene inactivity. Nature (London) **315**:594–597.
29. **Jenkins, N. A., and G. M. Cooper.** 1980. Integration, expression, and infectivity of exogenously acquired proviruses of Rous-associated virus-0. J. Virol. **36**:684–691.
30. **Kioussis, D., E. Vanin, T. deLange, R. A. Flavell, and F. G. Grosveld.** 1983. Globin gene inactivation by DNA translocation in gamma beta-thalassaemia. Nature (London) **306**:662–666.
31. **Linial, M., N. Gunderson, and M. Groudine.** 1985. Enhanced transcription of c-myc in bursal lymphoma cells requires continuous protein synthesis. Science **230**:1126–1132.
32. **Neel, B. G., G. P. Gasic, C. E. Rogler, A. M. Skalka, G. Ju, F. Hishinuma, T. Papas, S. M. Astrin, and W. S. Hayward.** 1982. Molecular analysis of the c-*myc* locus in normal tissue and in avian leukosis virus-induced lymphomas. J. Virol. **44**:158–166.
33. **Robinson, H.** 1979. Inheritance and expression of chicken genes which are related to avian-leukosis sarcoma viruses. Curr. Top. Microbiol. Immunol. **83**:1–36.
34. **Scholl, D. R., S. Kahn, S. Malavarca, S. Astrin, and A. M. Skalka.** 1983. Nucleotide sequence of the long terminal repeat and flanking cellular sequences of avian endogenous retrovirus *ev*-2: variation in Rous-associated virus-0 expression cannot be explained by differences in primary sequence. J. Virol. **45**:868–871.
35. **Schubach, W., and M. Groudine.** 1984. Alteration of c-myc chromatin structure by avian leukosis virus integration. Nature (London) **307**:702–708.
36. **Skalka, A., P. DeBona, F. Hishinuma, and W. McClements.** 1980. Avian endogenous proviral DNA: analysis of integrated

ev-1 and a related $gs^{-}chf^{-}$ provirus purified by molecular cloning. Cold Spring Harbor Symp. Quant. Biol. **44**:1097–1104.
37. **Spofford, J. B.** 1976. Position effect variegation in *Drosophila*, p. 955–1018. *In* M. Ashburner and E. Novitski (ed.), The genetics and biology of *Drosophila*, vol. 1C. Academic Press, Inc., New York.
38. **Stalder, J., M. Groudine, J. B. Dodgson, J. D. Engel, and H. Weintraub.** 1980. Hb switching in chickens. Cell **19**:973–980.
39. **Stuhlmann, H., D. Jahner, and R. Jaenisch.** 1981. Infectivity and methylation of retroviral genomes is correlated with expression in the animal. Cell **26**:221–232.
40. **Thompson, C. B., P. B. Challoner, P. E. Neiman, and M. Groudine.** 1985. Levels of c-myc oncogene mRNA are invariant throughout the cell cycle. Nature (London) **314**:363–366.
41. **Thompson, C. B., P. B. Challoner, P. E. Neiman, and M. Groudine.** 1986. Expression of c-myb proto-oncogene during cellular proliferation. Nature (London) **319**:374–380.
42. **Weintraub, H., A. Larsen, and M. Groudine.** 1981. α-Globin gene switching during the development of chicken embryos: expression and chromosome structure. Cell **24**:333–344.